University of Tasmania Open Access Repository

Cover sheet

Lithogeochemical halos and geochemical vectors to stratiform sediment hosted Zn–Pb–Ag deposits Part 2. HYC deposit, McArthur River, Northern Territory

Ross R. Large *, Stuart W. Bull, Peter J. McGoldrick

Centre for Ore Deposit Research, University of Tasmania, G.P.O. Box 252-79, Hobart, TAS 7001, Australia

Abstract

The giant stratiform Zn–Pb–Ag HYC deposit displays a broad Zn, Pb and Tl halo which extends laterally along the favourable pyritic black shale facies of the Barney Creek Formation for at least 15 km west of the deposit. A ferroan dolomite/ankerite halo overlaps with the Zn–Pb–Tl halo extending up to 250 m into the immediate stratigraphic hangingwall, and 50 to 100 m into the footwall sediments close to the deposit. A manganese carbonate halo is offset from the ferroan dolomite/ankerite halo, being concentrated in the immediate footwall of the deposit and extending laterally along the W-Fold Shale Member. Manganiferous carbonate forms the most pronounced and laterally extensive halo at HYC extending well beyond the Zn–Pb–Tl and ankerite halos. The geometry and extent of the halos described above are based on sampling and analyses from two drill holes reported in this study and a further six drill holes reported previously by I.B. Lambert and K.M. Scott [J. Geochem. Explor. 2, 307–330, 1973]. The SEDEX alteration index previously proposed as a vector for the Lady Loretta deposit [R.R. Large and P.J. McGoldrick, 1998, J. Geochem. Explor. 63, 37–56] has been shown to have applications in the McArthur Basin for defining the favourable stratigraphic unit hosting stratiform Zn–Pb–Ag mineralisation. A modified alteration index (AI Mark 3) has also been developed which eliminates the effect of the shale/dolomite ratio on the index and thus highlights the control of carbonate chemistry and its relationship to stratiform mineralisation. The application of a group of indices including Zn, Pb, Tl, SEDEX alteration index, AI Mark 3 and manganese content of dolomite (MnO_d) is proposed for defining the most favourable stratigraphic units for stratiform Zn–Pb–Ag mineralisation within carbonate-bearing sedimentary basins. © 2000 Elsevier Science B.V. All rights reserved.

Keywords: SEDEX; alteration index; zinc–lead; lithogeochemistry; halo; HYC

1. Introduction

Recent studies on the Proterozoic stratiform Zn–Pb–Ag deposit at Lady Loretta, Queensland (Large and McGoldrick, 1998) have enabled the development of a lithogeochemical halo model including quantifiable geochemical vectors that are potentially useful in mineral exploration. Three geochemical vectors were proposed.

(1) SEDEX metal index $= Zn + 100 Pb + 100 Tl$

(2) SEDEX alteration index $= (FeO + 10 MnO) \times 100/(FeO + 10 MnO + MgO)$

(3) Manganese content of dolomite: $MnO_d = MnO \times 30.41/CaO$.

At Lady Loretta all three vectors increase towards the ore lens both across and along strike. The useful-

---

ness of these vectors is dependent on the fact that the stratiform Zn–Pb–Ag mineralisation at Lady Loretta was accompanied by widespread dispersion of Zn, Pb and Tl along the favourable sedimentary host unit, and that the chemistry of carbonate minerals in the host sedimentary rocks change progressively from dolomite to ferroan–manganiferous dolomite to manganiferous siderite as the orebody is approached along and across the strata.

The work presented here aims to characterise the lithogeochemical halo to the much larger HYC deposit at McArthur River and to test the applicability of the geochemical vectors previously developed for the Lady Loretta deposit.

2. HYC Zn–Pb–Ag deposit

The HYC deposit is the largest and least deformed of the Proterozoic SEDEX deposits of northern Australia (Fig. 1), having a total geological resource of 237 million tonnes at 9.2% Zn, 4.1% Pb, 41 g/t Ag and 0.2% Cu (Gustafson and Williams, 1981). The
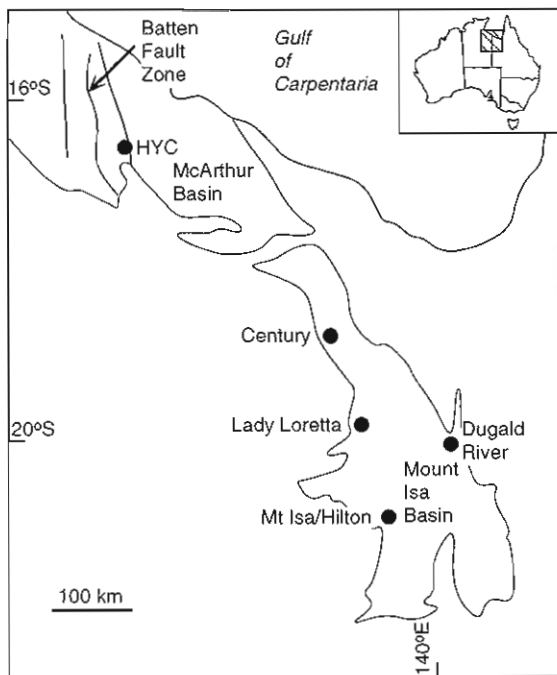
Fig. 1. Location of HYC deposit, in the McArthur Basin and other Proterozoic Zn–Pb SEDEX deposits in the Mt Isa Basin.
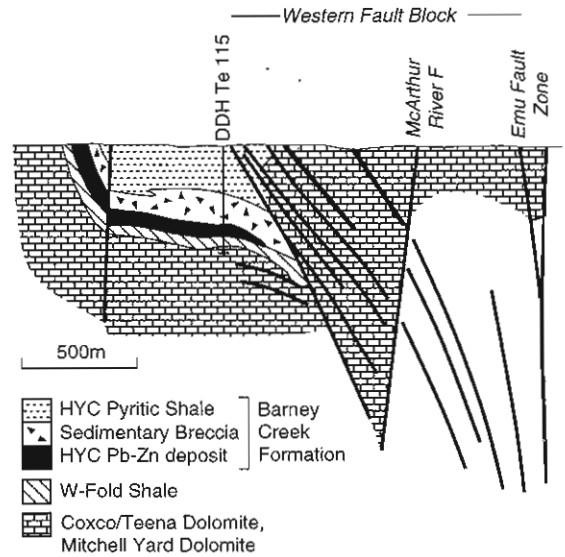
HYC GEOLOGY 182900N

Fig. 2. HYC deposit geology cross-section (from Hinman, 1995). Position of DDH Te 115 is projected 800 m north onto this section.

deposit consists of eight stacked ore lenses within the Barney Creek Formation (Fig. 2), a black shale-rich facies of the carbonate- dominated McArthur Group. Underground mining of the number 2 and 4 orebodies commenced in 1996.

The deposit is located adjacent to the regionally extensive Emu Fault (Figs. 2 and 3) which forms the eastern margin of the Batten Fault Zone, within the centre of the McArthur Basin (Fig. 1). The Emu Fault is considered to have acted as the conduit for mineralising sedimentary brines entering the basin (Brown et al., 1978; Williams, 1978). The eight separate ore lenses range from 1 to 5 m thick and are separated by dolomitic sedimentary breccias and pyritic dolomitic black shale. The breccias range in thickness from less than 30 cm to over 3 m and have been interpreted as slump breccias and graded turbidites related to movement along the Emu Fault system (Lambert, 1976; Walker et al., 1977; Logan, 1979; Large et al., 1998).

Within the ore lenses the Zn–Pb is concentrated in thin sphalerite–galena laminations (100 to 700 μm thick) separated by quartz–illite–carbonate silt layers and pyrite-rich organic mud layers (Large et al., 1998). Genetic models proposed for the deposit range from sedimentary–exhalative (Croxford and
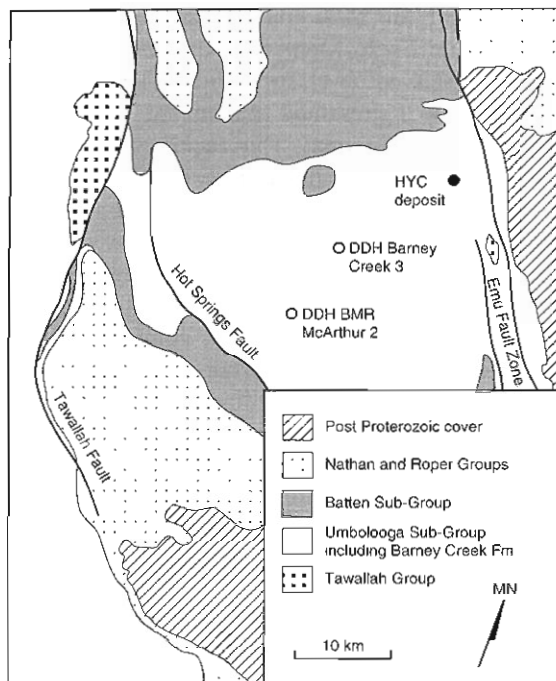
Fig. 3. Location of drill holes BMR 2 and Barney 3, with respect to HYC deposit and extent of the Umbolooga Sub-Group containing the Barney Creek Formation.

Jephcott, 1972; Lambert, 1976) to syn-diagenetic subsurface replacement (Williams, 1978; Eldridge et al., 1993; Hinman, 1995, 1996). Recent studies by Large et al. (1998) favour a syn-sedimentary model related to cycles of seismic pulse activity along the Emu Fault causing exhalation of dense metalliferous brines and accompanying mineral precipitation interspersed with turbidite sedimentation and pelagic organic mud deposition to give the finely laminated stratiform ore lenses.

3. Previous halo geochemical studies at HYC

Lambert and Scott (1973) undertook a detailed study of mineral dispersion within and surrounding the HYC deposit, and their geochemical database (Corbett et al., 1975) has proved to be an invaluable resource for this investigation. In their study, Lambert and Scott analysed 160 whole rock samples taken from eight diamond drill holes — two within the HYC deposit, two just beyond the boundaries of

the deposit and four at various distances from 2.5 to 23 km away. Lambert and Scott (1973) concluded from their study that favourable areas for HYC type deposits should contain: (1) pyritic, high-K carbonaceous shales; (2) anomalous Zn, Pb, Ag, Hg in shales; (3) dolomites with moderate to high Fe and Mn; and (4) vitroclastic tuff bands. They also showed that the Fe content of dolomites increased towards the HYC deposit and that the Mn content of the sediments is highest in the immediate footwall of the deposit. This study builds on the previous work of Lambert and Scott (1973) with particular emphasis on testing the geochemical vectors established at Lady Loretta (Large and McGoldrick, 1998).

4. Sampling and analysis

Sampling in this study was confined to two drill holes, DDH Barney 3 and DDH BMR 2, to the southwest of HYC (Fig. 3). Geochemical data for these holes were compared to data from six other drill holes, including DDH Te 115 through the HYC ore sequence, provided by Lambert and Scott (1973) and Corbett et al. (1975). Detailed sedimentological logs were constructed for both regional drill holes (Fig. 4) and samples where collected at 5 to 10 m intervals through the drilled sequence of Reward Dolomite, Barney Creek Formation and W-Fold Shale. Each sample was analysed for the complete set of major elements (SiO_2, TiO_2, Al_2O_3, FeO_{total}, MnO, MgO, CaO, N_2O, K_2O, P_2O_5, CO_2, S) and selected minor and trace elements. Sample preparation and analytical methods for DDH Barney 3 were the same as those outlined in our previous study at Lady Loretta (Large and McGoldrick, 1998). Samples collected by S. Bull from DDH BMR2 were analysed by AGSO Laboratories, Canberra, using techniques described in Cruikshank and Pyke (1993).

5. Host rock lithofacies and mineralogy, Barney Creek Formation

5.1. Host rock sedimentary facies

Bull (1998) provides a detailed account of the sedimentology of the 122 m long diamond drill
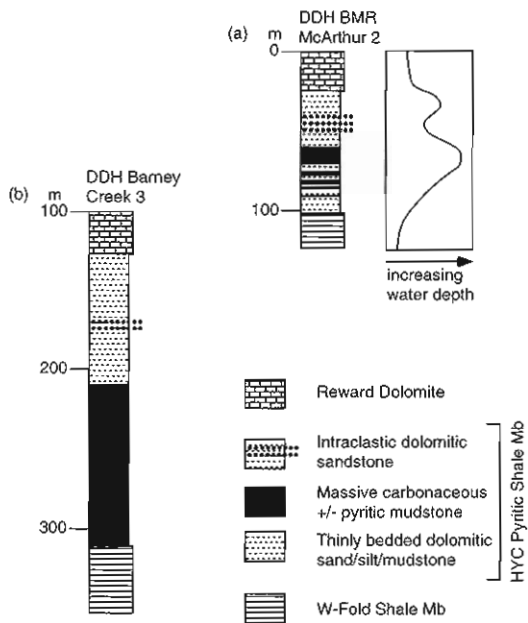
Fig. 4. Sedimentology logs for (a) DDH BMR 2 and (b) DDH Barney Creek 3 used in this study.

core DDH BMR 2 (Fig. 3) sampled in this study. It was collared in and intersected 25 m of Reward Dolomite, and terminated in the Barney Creek Formation after penetrating 82 m interpreted as HYC Pyritic Shale Member and 15 m interpreted as W-Fold Shale Member (Fig. 4a). Detailed sedimentary analysis indicated the presence of four sedimentary facies.

The dominant facies is thinly bedded dolomitic sandstone/siltstone/mudstone characterised by interbedded pale grey dolomitic siltstone/fine-grained sandstone beds and massive, grey/black (carbonaceous) mudstone. The dolomite beds represent small-volume, turbulent mass-flow deposits. The interbedded massive grey/black mudstone represents ambient depositional conditions. These involved the accumulation of fine-grained material from hemi-pelagic suspension in a quiet, reduced, sub-wave base subaqueous environment.

Thicker, discrete fine-grained intervals termed massive carbonaceous ± pyritic mudstone facies are also recognised. These have gradational contacts with the adjacent thinly bedded dolomitic sandstone/siltstone/mudstone facies, and are also interpreted as suspension deposits. Intervals of this

facies, which are most common at the base of the HYC Pyritic Shale Member, are considered to be relatively 'starved' of clastic sediment input, and are interpreted to represented maxima of water depth and/or shoreline retreat. This facies is host to the stratiform Zn–Pb–Ag mineralisation at HYC.

An intraclastic dolomitic sandstone facies is represented by isolated coarse-grained to very coarse-grained beds. These units are interpreted as mass flows sourced from erosion in an agitated shoreline environment of either older, competent, structurally elevated McArthur Group units, or shallow (exhumed) or surficial early diagenetic crusts. Units of this facies are thickest, coarsest and most abundant in the upper middle part of the HYC Pyritic Shale Member intersection from 53 to 38 m in DDH BMR2, and this interval is interpreted to represent a period of shallowing and/or shoreline retreat (Bull, 1998).

A laminated and rippled grey dolomite facies comprises the uppermost 25 m of the drill hole and is considered to represent the Reward Dolomite. Subtle but important differences to the underlying Barney Creek Formation intersection include, a lower proportion of mudstone and a marked increase in tractional sedimentary structures such as ripples and scours.

Interpretation of the facies defined in the Barney Creek Formation interval intersected in DDH BMR 2 (Bull, 1998) indicates that the succession was deposited entirely within a quiet, reduced, sub-wave base environment. However, the restriction of key facies to discrete stratigraphic intervals indicates subtle fluctuations in environmental conditions, chiefly water depth, during deposition. A schematic relative water depth curve has been constructed (Fig. 4a; Bull, 1998) that identifies two periods of increasing water depth (one from the W-Fold Shale Member into the lower part of the HYC Pyritic Shale Member, and one in the upper part of the HYC Pyritic Shale Member), and two periods of shallowing and/or shoreline transgression (one in the middle/upper part of the HYC Pyritic Shale Member and one at the top of the hole, representing a gradational contact between the Barney Creek Formation and the Reward Dolomite).

Logging and sampling of DDH Barney Creek 3 was conducted from 100 m below the collar to the

end of the hole at 353 m (Fig. 4b). This interval consists of 27 m of Reward Dolomite and 240 m of Barney Creek Formation comprising 184 m of HYC Pyritic Shale and 42 m of W-Fold Shale. The drill core is extensively fractured and disrupted, particularly in the bottom half of the drill hole, making detailed sedimentological analysis difficult. It is clear though, that while the HYC Pyritic Shale Member intersection is thicker, all three facies recognised in the unit in DDH BMR 2 are present (Fig. 4b), indicating that the overall depositional setting is the same. In addition, the facies are arranged in a similar manner in that the massive carbonaceous ± pyritic mudstone facies is dominant in the lower half, and a thin zone consisting of thick intraclastic dolomitic sandstone beds is present in the upper middle part. This suggests that in spite of the greater overall thickness of the intersection, and thicker and more massive development of the carbonaceous ± pyritic mudstone facies in DDH Barney Creek 3, which are thought to reflect a position closer to the centre of the sub-basin that hosts the HYC deposit, the relative water depth history is similar to that proposed for DDH BMR 2 (Fig. 4a).

The diamond drill core DDH Te 115 was logged by Brown et al. (1978). It was collared and terminated in Barney Creek Formation and consists of 452 m of HYC Pyritic Shale Member and 80 m of W-Fold Shale Member. The graphic log presented by Brown et al. (1978) is difficult to interpret in terms of the facies scheme presented by Bull (1998). Because the core was not available for re-logging by the authors no sedimentological interpretation is presented here.

5.2. Host rock mineralogy

Sedimentary rocks of the Barney Creek Formation have a relatively simple mineralogy of carbonate (dolomite, ankerite), illite, quartz, K-feldspar, pyrite with trace chlorite and organic matter. Carbonate content of the carbonaceous pyritic mudstone facies host to the mineralisation ranges from 1 to 40 wt% (Fig. 5a), but high-grade mineralisation is generally associated with sedimentary intervals containing less than 10 wt% carbonate. The thinly bedded dolomite siltstone facies ranges from 30 to 60 wt% carbonate, while the dolomitic sandstone and sedimentary
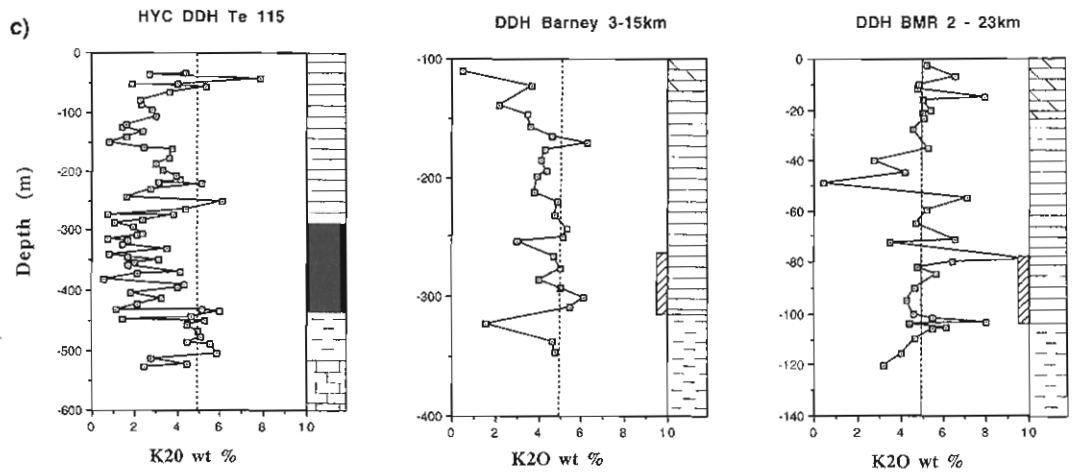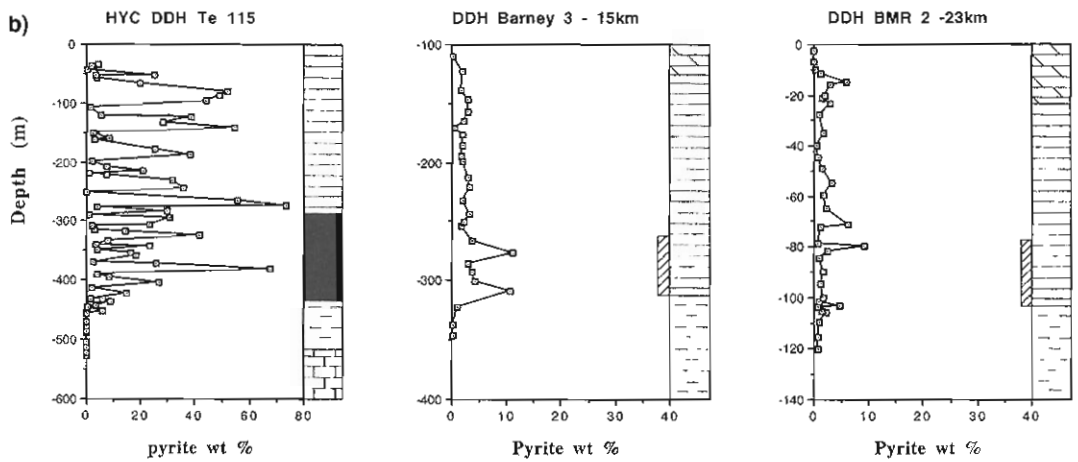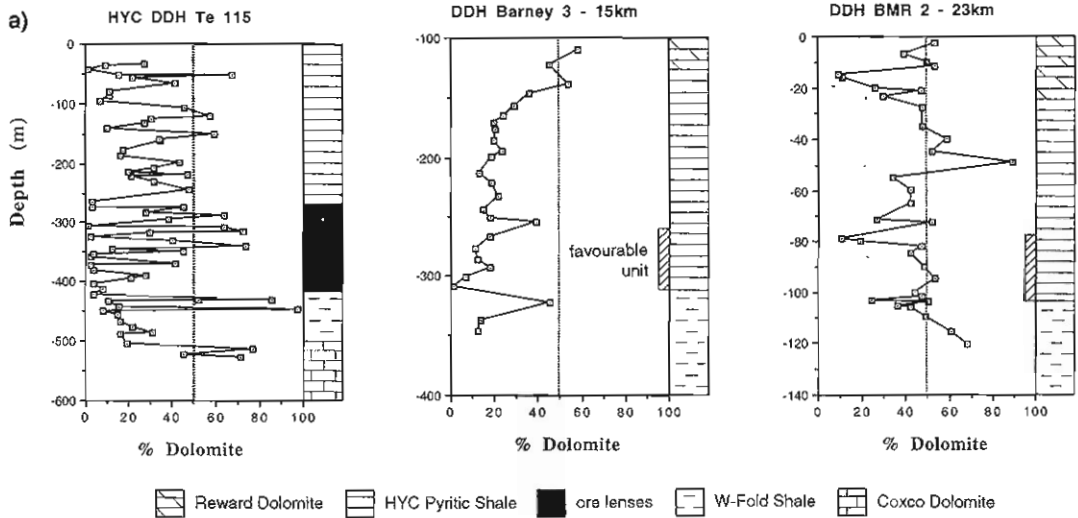
breccia facies typically contain greater than 50 wt% carbonate. Whole rock chemistry and microprobe studies (discussed later) indicate that dolomite and ferroan dolomite/ankerite are the only major carbonate minerals present. Calcite occurs rarely and siderite has not been identified either at HYC or regionally within the McArthur Basin.

The pyrite content of Barney Creek Formation varies considerably across the basin, and within the three drill holes studied (Fig. 5b). At HYC the pyrite content of the HYC Pyritic Shale Member ranges from 10 wt% to more than 90 wt% with the pyrite concentrated in thin bands parallel to bedding. Downhole plots of total pyrite content of the sedimentary rocks calculated from FeO and S analyses indicate that strongly pyritic shales extend up to 200 m above the orebody, but there is a sharp drop to less than 1 wt% pyrite in W-Fold Shale below the deposit. In the Barney Creek Formation, intersected in DDH Barney 3, 15 km southwest of HYC, pyrite content generally ranges from 1 to 5 wt%, with two narrow intervals at the base of the formation (280–310 m downhole) reaching up to 10 wt% pyrite. Twenty-three km distant at DDH BMR 2 pyrite content of the Barney Creek Formation varies irregularly from 0.7 to 10 wt% with no discernible pattern.

Downhole K_2O variation (Fig. 5c) is controlled by illite and K-feldspar distribution within the sediments. XRD and petrographic studies indicate that illite is the dominant potash mineral around the ore zone where the sediments range from 0.5 to 4 wt% K_2O. In DDH Barney 3 the sedimentary rocks contain a mixture of illite and K-feldspar, while remote from HYC in DDH BMR 2, K-feldspar is the dominant potash mineral, and the sedimentary rocks typically contain levels of K_2O from 4 to 8 wt%. Davidson (1998) has recognised several phases of potash metasomatism within sediments of the McArthur Group, the main regional phase being possibly related to decent of saline fluids which form the recharge zone of the HYC hydrothermal system (Davidson, 1998).

6. Halo of ore-related elements

Our data support those of Lambert and Scott (1973) which showed an extensive halo of Zn and Pb

extending into the hangingwall pyritic shales above the ore lenses and along the base of the HYC Pyritic Shale Member laterally from the deposit.

6.1. Zinc

Distal from the orebody in the upper parts of the Barney Creek Formation and lower Reward Dolomite, background Zn values range from 5 to 100 ppm (Fig. 6a). In DDH Te 115 through the deposit, Zn increases abruptly at the base of the HYC Pyritic Shale to values over 10,000 ppm; however, inter-ore dolomitic siltstone and breccia contain between 100 and 10,000 ppm Zn. Zinc values from 100 to 20,000 ppm persist for 250 m into the overlying HYC Pyritic Shale (Fig. 6a; Lambert and Scott, 1973). At 15 km to the southwest of HYC, anomalous Zn values above 1000 ppm are restricted to a 40 m interval toward the base of the HYC Pyritic Shale in DDH Barney 3. This is interpreted to be the HYC stratigraphic position. There is a general increase in Zn from 5 ppm to 100 ppm over the 150 m interval of the hangingwall shales approaching the ore position. In DDH BMR 2, 23 km distant from HYC, the thickness of the Barney Creek Formation is considerably reduced (<100 m compared with 440 m at HYC and 200 m at DDH Barney 3), and no anomalous Zn was defined at the base of the formation. An anomalous Zn zone (100–1000 ppm) at 45 to 65 m downhole (Fig. 6a) does not correspond to any sedimentological or other lithogeochemical feature and is considered to be unrelated to the HYC mineralisation. Combining our data with those of Lambert and Scott (1973) indicates that a Zn halo of greater than 1000 ppm extends west from HYC along the base of the HYC Pyritic Shale for at least 15 km.

6.2. Lead

The distribution of Pb in the sedimentary rocks surrounding HYC is similar to that of Zn but with a lower order of magnitude. Lead values of 5 to 50 ppm occur in sediments distal from HYC (DDH BMR 2), while a halo of greater than 100 ppm Pb is confined to the base of the HYC Pyritic Shale along the ore position, as shown in DDH Barney 3 (Fig. 6b). No major Pb anomalies are evident in DDH BMR 2, 23 km west of HYC.

6.3. Copper, arsenic and barium

Although Cu is only present in minor amounts in the HYC ore (0.1–0.5 wt%), it exhibits a similar distribution pattern to Pb and Zn. Background Cu values in the Barney Creek Formation in the distal hole BMR 2 are between 2 and 30 ppm, increasing to values between 30 and 80 ppm at the base of the HYC Pyritic Shale in DDH Barney 3.

Arsenic closely follows pyrite distribution (Lambert and Scott, 1973) in the three drill holes studied reaching values of 1000–2000 ppm through the ore zone but decreasing to 100–800 ppm at the base of the HYC Pyritic Shale in DDH Barney 3.

Barium shows no correlation with the ore metals, commonly ranging from 100 to 600 ppm throughout the HYC Pyritic Shale. However, there is a good linear correlation with K_2O, indicating that Ba substitutes for K in illite and K-feldspar within the Barney Creek Formation sediment.

6.4. Thallium

Recent studies of the Lady Loretta SEDEX deposit (Large and McGoldrick, 1998) have shown that Tl is widely dispersed in the sediments hosting the deposit, forming a more extensive halo than either Zn or Pb. Limited analyses on DDH Te 115 at HYC by Smith (1973) are compared with our data from DDH Barney 3 and DDH BMR 2 in Fig. 6. Through the ore zone in DDH Te 115, Tl ranges from 100 to 1000 ppm while distal from the deposit background values are commonly less than 4 ppm (upper parts of DDH Barney 3 and DDH BMR 2). Using a 4 ppm

Fig. 5. Downhole variation of (a) dolomite, (b) pyrite, and (c) K_2O for the three holes studied. Dolomite content is calculated from CaO analyses assuming all CaO is present in dolomite. Pyrite content is calculated from S analyses, after excluding for S present in base metal sulphides. The dotted lines at 50% dolomite and 5% K_2O are shown to enable easy comparisons between drill holes. The favourable unit marked in DDH Barney 3 and DDH BMR is the along strike correlation of the ore zone in DDH Te 115.
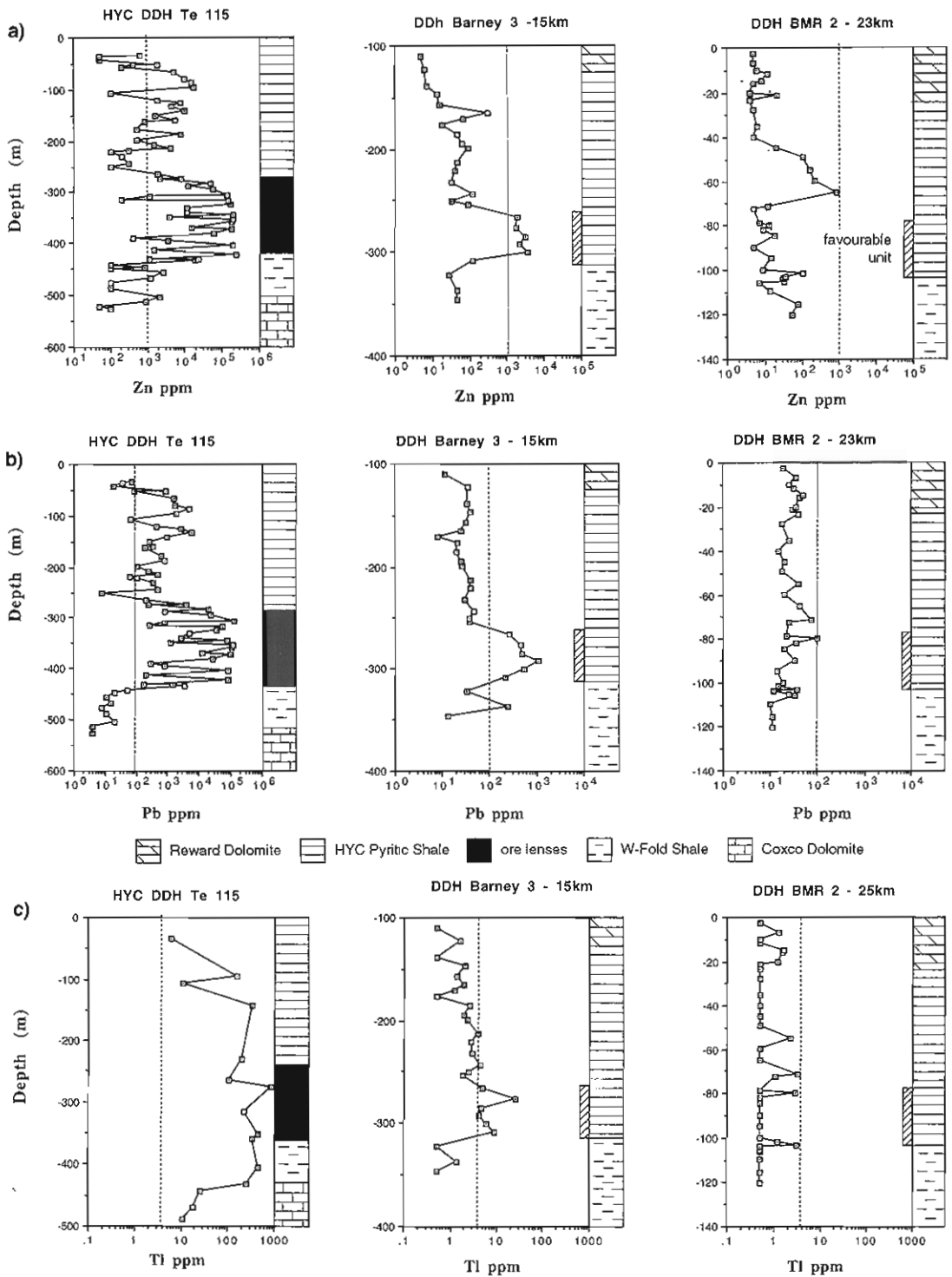
Fig. 6. Downhole variation of (a) Zn, (b) Pb, and (c) Tl for the three holes studied. The dotted lines marking 1000 ppm Zn, 100 ppm Pb and 4 ppm Tl are shown to enable easy comparisons between drill holes, and are not considered to be threshold values.

threshold, all samples in DDH Te 115 are considered to be anomalous, suggesting that a broad Tl halo surrounds the deposit extending at least 250 m into the hangingwall and 100 m into the footwall. In DDH Barney 3, anomalous Tl (>4 ppm) is restricted to the interpreted ore position at the base of the HYC Pyritic Shale. A downward trend of increasing Tl from 0.5 to 4 ppm occurs in the hangingwall approaching the ore position (Fig. 6c) and parallels the trend of Zn over the same interval. No anomalous Tl is present in DDH BMR 2, suggesting that the Tl halo to HYC does not extend to this drill hole.

6.5. Metal index

Large and McGoldrick (1998) proposed a metal index combining Pb, Zn and Tl in the following way as a vector to SEDEX deposits.

$$\text{Metal index} = \text{Zn} + 100\,\text{Pb} + 100\,\text{Tl} \quad (\text{in ppm}) \quad (1)$$

This combination accounts for the widespread dispersion of Tl and tight dispersion of Pb, forming an index that should increase systematically towards ore. Applying this index to the three drill holes in the McArthur Basin (Fig. 7) shows that the orebody is characterised by values greater than 10^6, with an extensive hangingwall halo of values greater than 10^4. In DDH Barney 3, 15 km west of HYC, the

metal index clearly defines the ore position with values greater than 10^4, peaking at around 10^5. In DDH BMR 2, no clearly anomalous values are evident, with a maximum of 10^4 at 80 m downhole (25 m above the base of the HYC Pyritic Shale).

7. Halo of carbonate minerals

Previous whole rock analyses and carbonate staining studies at HYC (Lambert and Scott, 1973) indicated that both the Fe and Mn content of carbonates within the Barney Creek Formation decrease away from the HYC deposit. A similar pattern was defined at the Lady Loretta SEDEX deposit (Carr, 1984; Large and McGoldrick, 1998), with our recent research defining successive halos of carbonate minerals surrounding the deposit: an inner halo of manganiferous siderite siltstones, followed by an outer halo of manganiferous ankerite/ferroan dolomite which merges with low-Fe–Mn dolomitic sediments representing the regional background of the Lady Loretta Formation. Further work was undertaken on the sedimentary rocks surrounding HYC, as part of this study, in order to quantify the Mn- and Fe-carbonate relationships and distribution, and compare these with the sedimentary facies and metal halos discussed previously.
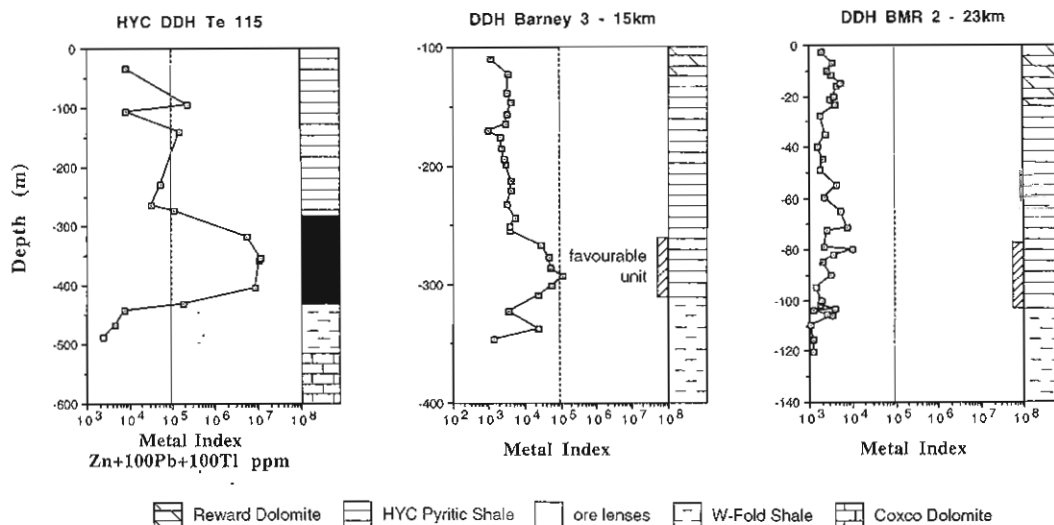

Fig. 7. Variation in metal index (Zn + 100 Pb + 100 Tl) down the three drill holes Te 115, Barney 3 and BMR 2.
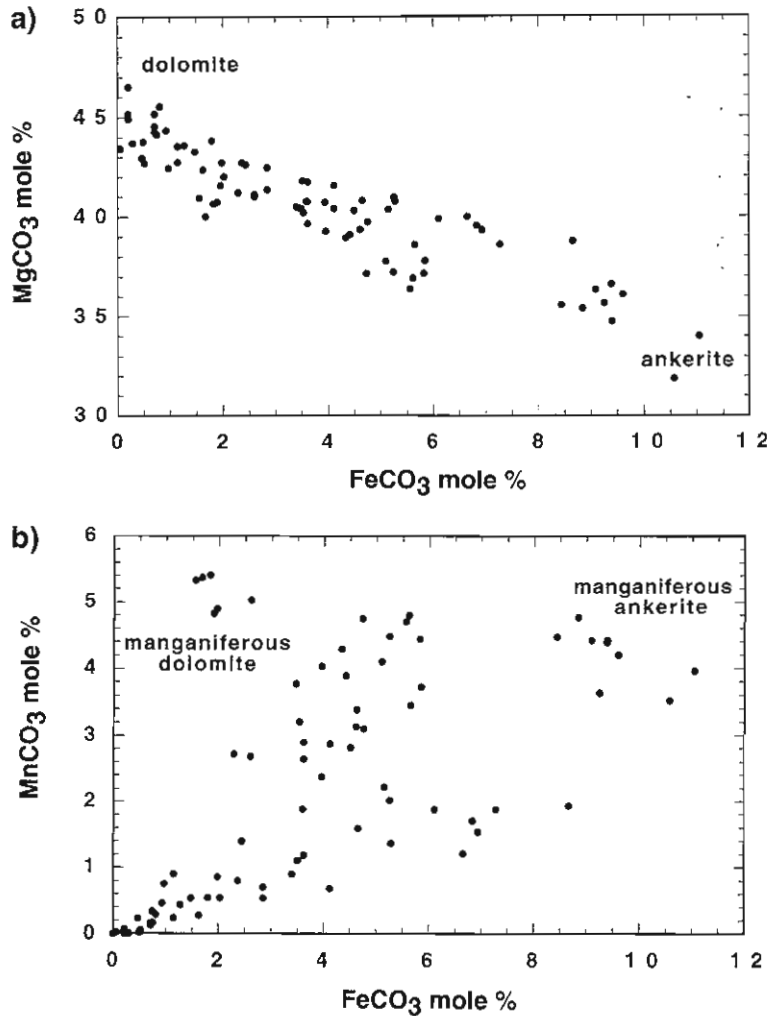
Fig. 8. Microprobe analyses of carbonate grains from five selected samples in DDH Barney 3: (a) shows the variation from dolomite to ankerite; (b) shows the degree of Mn and Fe substitution for Mg in the dolomite structure.

7.1. Carbonate chemistry

Eldridge et al. (1993) report three types of carbonate in the ore zones at HYC: (1) clean dolomite in the unmineralised sediments; (2) ferroan dolomite in the mineralised nodular dolomite zones; and (3) coarse rhombohedral ankerite within the sphalerite–galena bands. Microprobe analyses on six selected dolomitic sediment samples in DDH Barney 3 (Fig. 8; Table 1) show that the sedimentary carbonate ranges in composition from relatively pure dolomite (upper HYC Pyritic Shale) to ankerite/ferroan dolomite (lower HYC Pyritic Shale) and manganiferous ferroan dolomite (W-Fold Shale).

7.2. Manganese carbonate halo

Data from DDH Te 115 (Corbett et al., 1975) show strong Mn enrichment in the W-Fold Shale dolomitic sedimentary rocks immediately below the ore deposit, with values from 0.5 to 1.7 wt% MnO (Fig. 9a). Within the ore zone, MnO values are less than 0.5 wt%, but an interval of weakly elevated MnO (0.5–0.8 wt%) occurs at the top of the ore-

Table 1

Selected microprobe analyses of sedimentary carbonates (mole%) from DDH Barney 3, 15 km west of the HYC deposit (these five analyses were selected from a database of 82 microprobe analyses)

	123 R3C1	338 R1C4	293 z x	322 R3GM4	322 R2C1
$CaCO_3$	54.21	52.35	51.12	53.82	51.85
$MgCO_3$	44.14	40.73	39.11	31.88	40.96
$FeCO_3$	0.75	3.95	4.41	10.58	1.56
$MnCO_3$	0.17	2.38	3.89	3.52	5.33
Total	99.27	99.41	98.53	99.80	99.70

123 R3C1 = dolomite from top of HYC Pyritic Shale; 338 R1C4 = weakly Fe–Mn dolomite from W-Fold Shale; 293 z x = Fe–Mn dolomite from base of HYC Pyritic Shale; 322 R3GM4 = Fe-rich dolomite from top of W-Fold Shale; 322 R2C1 = Mn-rich dolomite from top of W-Fold Shale.

body and extends into the hangingwall sediments. The upper HYC Pyritic Shales are devoid of significant MnO (<0.25 wt%). To the west of HYC, MnO shows mild enrichment at the top of the W-Fold Shale in both DDH Barney 3 (maximum 1.0 wt% Mn) and DDH BMR 2 (maximum 0.5 wt% Mn). Microprobe analyses (Fig. 8; Table 1) show that Mn occurs in the sediments as manganiferous dolomite and manganiferous ankerite. Using the whole rock MnO and CaO analyses, it is thus possible to calculate the average MnO content of dolomite (or ankerite) in the sediments according to the following relationship defined by Large and McGoldrick (1998). MnO content of dolomite:

$$MnO_d = \frac{MnO_{wr} \times 30.41 \ [\text{wt\%}]}{CaO_{wr}} \qquad (2)$$

where MnO_{wr} and CaO_{wr} are the whole rock values.

This is a more useful parameter than whole rock MnO, as it is less affected by sedimentary facies and variations in carbonate content of the host sediment.
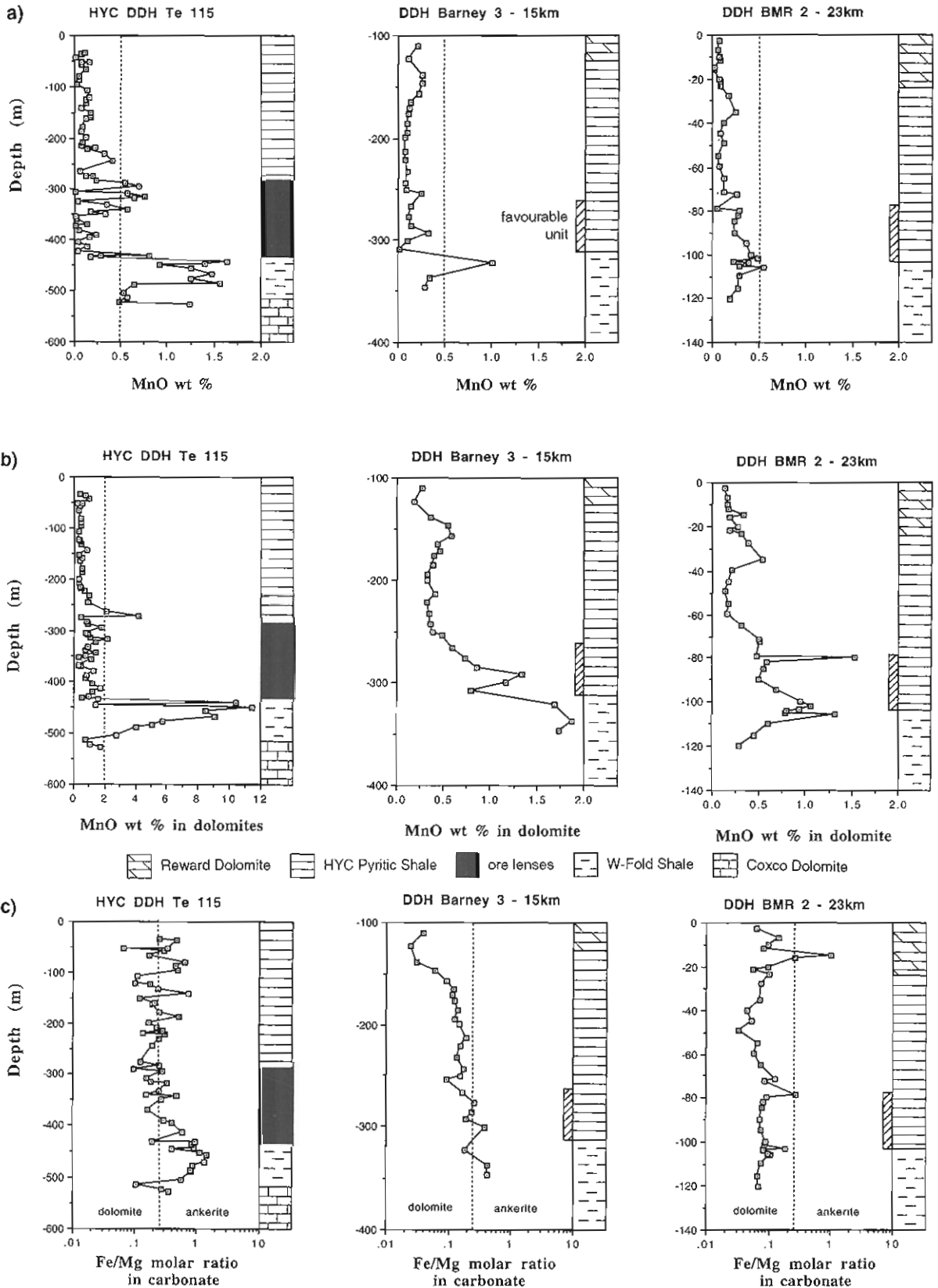
Downhole plots of MnO_d for all three drill holes (Fig. 9b) show a more systematic pattern of Mn in carbonate distribution and clearly define a Mn-rich carbonate halo below the HYC deposit. The maximum MnO content of dolomite reaches 12 wt% at the top of the W-Fold Shale immediately below the ore zone, and decreases systematically with depth through the footwall W-Fold Shale from 12 wt% to 1 wt% over an interval of 50 m. MnO_d values range from 0.2 to 0.4 wt% in sedimentary rocks of the upper Barney Creek Formation distal to the deposit. In DDH Barney 3 (Fig. 9b), MnO_d values increase systematically with depth over a distance of 100 m

passing stratigraphically down toward the base of the HYC Pyritic Shale. Maximum values of 1.5 to 2.0 wt% MnO in dolomite occur near the top of the W-Fold Shale below the interpreted ore position. In DDH BMR 2, peak MnO_d values of 1.2–1.5 wt% bracket the interpreted ore position at the base of the HYC Pyritic Shale. MnO_d increases from both the footwall and hangingwall sides toward the ore position from background values (≤0.25 wt%) up to 0.5 wt%.

In summary, a Mn halo, represented by anomalously high MnO values in dolomite within the sediments (MnO_d), has been traced from the orebody, along the footwall sedimentary sequence (W-Fold Shale Member), over a distance of 23 km west of the deposit to DDH BMR 2. Lithogeochemical data previously reported from six other drill holes in the vicinity of HYC by Lambert and Scott (1973) and Corbett et al. (1975) support the regional extent and continuity of this Mn halo.

7.3. Iron carbonate halo

In order to provide quantitative information about the variation in Fe content of carbonates at HYC, a computer program was developed to calculate the average molar ratio Fe/Mg for the carbonate component of the sediments utilising whole rock analyses. Downhole plots of this calculated molar ratio are shown in Fig. 9c. The following assumptions were made in calculating the ratio: (1) Dolomite and/or ankerite are the only carbonate minerals present. This was confirmed by plotting MgO vs CaO and CaO vs CO_2. More than 95% of carbonate-bear-

a) HYC DDH Te 115 — DDH Barney 3 - 15km — DDH BMR 2 - 23km; MnO wt %; favourable unit

b) HYC DDH Te 115 — DDH Barney 3 - 15km — DDH BMR 2 - 23km; MnO wt % in dolomites / MnO wt % in dolomite

Legend: Reward Dolomite | HYC Pyritic Shale | ore lenses | W-Fold Shale | Coxco Dolomite

c) HYC DDH Te 115 — DDH Barney 3 - 15km — DDH BMR 2 - 23km; Fe/Mg molar ratio in carbonate; dolomite / ankerite

ing samples studied from the McArthur Basin were found to be dolomitic. Calcite is rare and siderite is absent. (2) Pyrite, ferroan dolomite and ankerite are the only minerals containing significant Fe. Trace amounts of Fe present in sphalerite and chalcopyrite in the sediments have been ignored. (3) The only sulphide minerals are pyrite, sphalerite, galena and chalcopyrite. (4) Dolomite/ankerite is the only Mg-bearing mineral.

Trace amounts of chlorite in some samples contravenes assumptions 2 and 4 and may cause problems with the calculation, but this is considered to be of little significance for the McArthur Basin drill samples studied here. Selected microprobe analyses indicate that the calculated Fe/Mg molar ratios are consistently greater than the probe determined ratios, although they show the same downhole trends. The microprobe analyses also show considerable variability in Fe/Mg ratio, making it difficult to compare the individual microprobe analyses with those calculated from the whole rock data (which represent an average molar ratio for all carbonate grains in the sample analysed). On this basis the calculated data should be considered as semi-quantitative only.

From the downhole plots in Fig. 9c it is apparent that the most Fe-rich carbonates occur at the base of the ore zone in DDH Te 115, and the upper section of the W-Fold Shale below the deposit. Carbonate in the hangingwall pyritic shales ranges from ferroan dolomite to ankerite, but with lower Fe/Mg ratios than the ore zone.

Distal from the deposit in DDH Barney 3, the hangingwall pyritic shales contain ferroan dolomite, with ankerite predominant in the sedimentary rocks interpreted as correlative with the HYC ore zone and W-Fold Shale. At the remote location of DDH BMR 2, most sediments contain low-Fe dolomite with Fe/Mg molar ratios of 0.05 to 0.1. Spikes of elevated Fe/Mg ratio occur at 15 and 80 m downhole and correspond to beds of massive carbonaceous pyritic shale with low carbonate content.

In summary, this semi-quantitative approach using the whole rock analyses and supported by limited microprobe data suggests the existence of a ferroan

dolomite/ankerite halo, surrounding the orebody that extends as far west as DDH Barney 3. The halo is characterised by both ferroan dolomite and ankerite compositions with a variable Fe/Mg molar ratio of around 0.1 to 2.0.

7.4. Relationship of Fe-carbonate halo to Mn-carbonate halo

The ferroan dolomite halo and Mn-carbonate halo at HYC are roughly coincident; however, there are some important differences. Firstly, the ferroan dolomite halo around the deposit extends further into the hangingwall sedimentary rock than the Mn-carbonate halo. Secondly, the Mn-carbonate halo can be traced to DDH BMR 2, 23 km from the deposit, whereas the ferroan dolomite halo is less extensive, reaching to beyond DDH Barney 3 (15 km) but not as far as DDH BMR 2. Thirdly, the most Fe-rich ankerites are found in the ore zone, base of the HYC Pyritic Shale and top of the W-Fold Shale, whereas the most Mn-rich carbonates do not occur in the ore zone, but at the top of the W-Fold Shale in the footwall to the ore position.
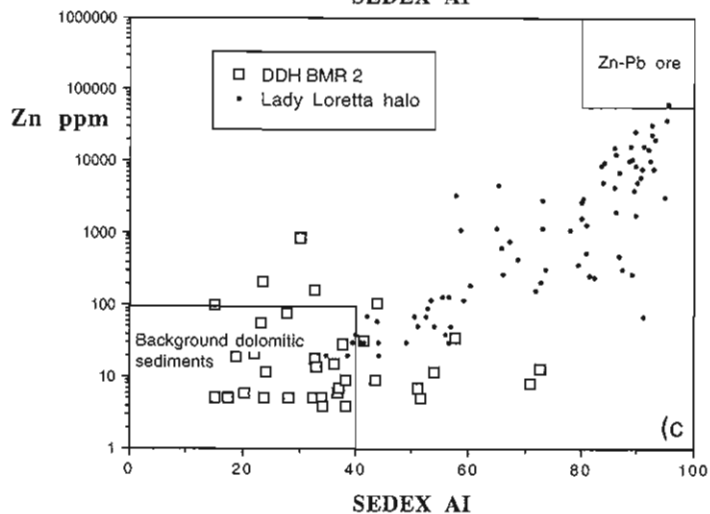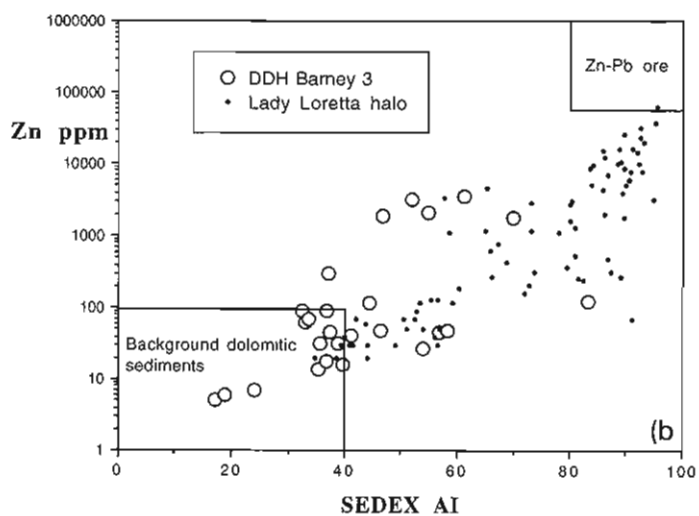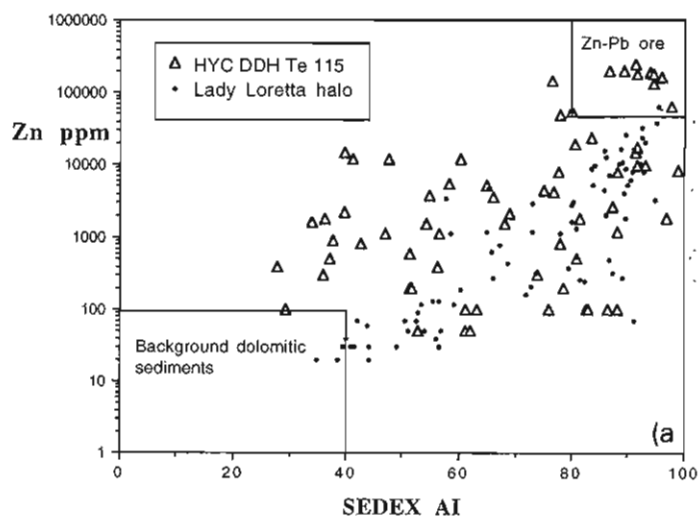
8. Application of the alteration index (SEDEX AI) to HYC

Our recent geochemical research at Lady Loretta (Large and McGoldrick, 1998) resulted in the development of an alteration index to assist in mapping halos surrounding SEDEX deposits and to provide a vector to ore:

$$SEDEX\ AI = \frac{100(FeO + 10\,MnO)}{FeO + 10\,MnO + MgO} \qquad (3)$$

The index relies on the changes in whole rock chemistry accompanying carbonate mineral chemistry variations associated with Zn–Pb–Ag mineralisation; FeO and MnO are enriched during development of Fe–Mn carbonate phases, while MgO is depleted due to replacement by FeO and/or MnO in the carbonate structure. The index ranges from

Fig. 9. Downhole plots of (a) MnO, (b) MnO content of dolomite (MnO_d), and (c) Fe/Mg molar ratio of carbonate. The MnO content of dolomite and Fe/Mg molar ratios were calculated from the whole rock analyses as described in the text.
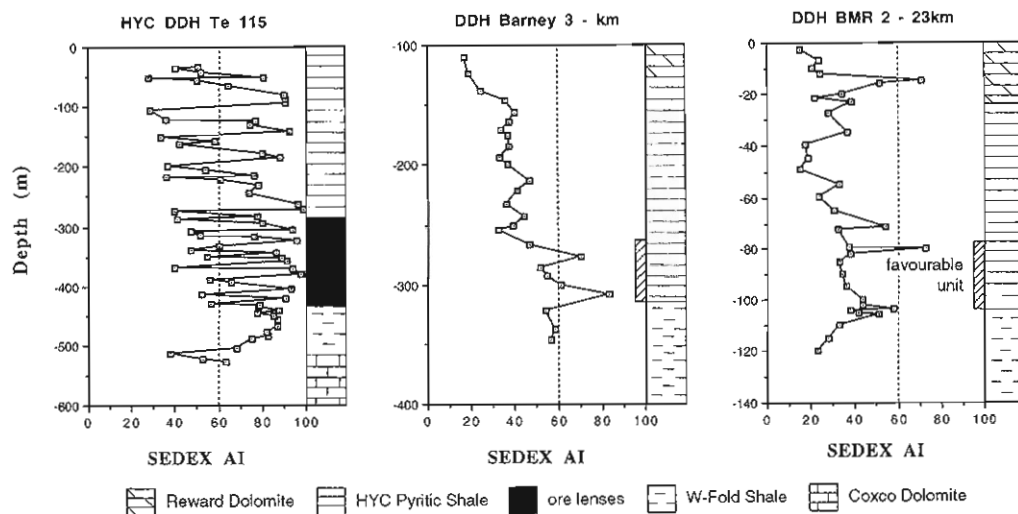
Fig. 11. Downhole variation of SEDEX AI for the three drill holes studied. The pattern in DDH Barney 3 clearly defines the favourable unit for stratiform Zn–Pb mineralisation.

values of 0 to 40 in background dolomitic sediments upwards to values of 80 to 100 in sediments directly associated with mineralisation. A trend of increasing SEDEX AI with increasing Zn mineralisation was proposed to characterise the sedimentary units hosting stratiform Zn–Pb–Ag mineralisation (Large and McGoldrick, 1998, fig. 13). Similar trends are evident in the sedimentary rocks hosting the HYC deposit (Fig. 10). Close to HYC in DDH Te 115, all the sediments have anomalous values of SEDEX AI > 40 or Zn > 100 ppm (Fig. 10a), with maximum AI (80–100) corresponding to maximum Zn within and close to the ore zone. Sediments in DDH Barney 3, at the outer limit of the ferroan dolomite/ankerite halo, show a similar trend of increasing AI with increasing Zn (Fig. 10b). A systematic increase in SEDEX AI from the top of the drill hole (110 depth) to the base of the HYC Pyrite Shale (300 m depth) provides an excellent vector to the ore-bearing stratigraphic position (Fig. 11).

Most samples from DDH BMR 2 plot within the background field in Fig. 10c, with SEDEX AI values of less than 40 and Zn values less than 100 ppm. Several spikes above 40 occur toward the base of the

HYC Pyritic Shale (Fig. 11c) and may relate to increased pyrite within the carbonaceous black shales in these intervals. Elevated SEDEX AI values at the top of the drill hole correspond to a carbonaceous unit at the base of the Reward Dolomite.

In summary, the SEDEX alteration index developed for Lady Loretta, also has application as a vector in the McArthur Basin. The index is elevated in the ferroan carbonate/ankerite halo immediately surrounding the deposits and increases towards ore through the hangingwall sedimentary rocks and along the favourable stratigraphy at the base of the HYC Pyritic Shale.

9. Modification of the alteration index

The SEDEX AI (Eq. 3) is affected by three major lithochemical factors associated with stratiform Zn–Pb–Ag deposits:

(1) *Carbonate factor*: changes in carbonate chemistry in the halo of the deposit; increasing Fe and Mn in carbonate causes increasing AI. This is the basis of the development of the index.

Fig. 10. (a–c) Variation in SEDEX alteration index with Zn in the three drill holes studied. The positive trend of increasing SEDEX AI with Zn content is characteristic of the halo to Proterozoic carbonate/shale hosted SEDEX deposits in Australia. The pattern for each drill hole is compared to that reported for the Lady Loretta deposit by Large and McGoldrick (1998).

(2) *Pyrite factor*: an increase in the pyrite content of sediments causes an increase in whole rock FeO and consequent increase in SEDEX AI (Eq. 3). This is a supporting factor for (1) above, as most SEDEX deposits are associated with pyritic shales.

(3) *Shale factor*: changes in shale/dolomite ratio cause a change in the whole rock MgO value and therefore a change in the SEDEX AI. Carbonaceous shales for example contain less dolomite, have lower MgO contents and consequently higher SEDEX AI values.

All three factors (Fe–Mn carbonate, pyrite and shale) increase in proximity to stratiform Zn–Pb in the Australian Proterozoic and this contributes to the use of SEDEX AI as a vector to ore. However, this also means that a change in sedimentary facies from dolomite to shale alone may give rise to anomalous alteration index values irrespective of whether or not they are related to a SEDEX deposits. Thus, as it stands, the index cannot discriminate 'barren' shale horizons from potentially fertile shale horizons within a dolomitic sedimentary basin. This problem is demonstrated in Fig. 12a where the SEDEX AI has been plotted against dolomite content for a set of 'barren' dolomitic sediments from the McArthur Basin. The data show a general trend of increasing SEDEX AI with decreasing dolomite content (i.e., increasing shale content) in the sediments.

Although it is useful to have a shale factor built into the alteration index, because of the importance of shale facies in hosting stratiform Zn–Pb ores, it is not desirable for the shale factor to become dominant to the extent that any shale in a dolomitic sequence causes an anomalous elevated response. In order to counterbalance the shale factor, a series of modifications to the alteration index have been investigated. Two of these modifications which were found to be successful in eliminating the shale factor are given below:

$$\text{AI Mark } 3 = \frac{100(\text{FeO} + 10\,\text{MnO})}{\text{FeO} + 10\,\text{MnO} + \text{MgO} + \text{Al}_2\text{O}_3}$$

for use in argillaceous dolomitic packages;

$$\text{AI Mark } 4 =$$

$$\frac{100(\text{FeO} + 10\,\text{MnO})}{(\text{FeO} + 10\,\text{MnO} + \text{MgO} + \text{SiO}_2/10)}$$

for use in siliciclastic dolomitic packages.

An increase in the shale/dolomite ratio in a sediment package is accompanied by decreasing MgO and increasing Al_2O_3, SiO_2 and K_2O. Consequently, introducing Al_2O_3 or SiO_2^- into the denominator of the alteration index provides a counterbalance to the effect of the shale component on the index. This is shown in Fig. 12b where the previous negative trend between dolomite content and SEDEX AI has been changed into a slightly positive trend between dolomite content and AI Mark 3. Fig. 12b shows that dolomite-rich sediments have a mean AI Mark 3 of about 20, while dolomite-poor shales have a mean AI Mark 3 of about 15. Whereas the background population for SEDEX AI was taken as 0 to 40 (Figs. 10 and 11), this has been reduced to 0 to 30 for AI Mark 3. A comparison between the pattern of SEDEX AI and AI Mark 3 in DDH Barney 3, 15 km west of HYC, is shown in Fig. 13. Both indices clearly define the potential ore position at the base of the HYC Pyritic Shale; however, the response from the AI Mark 3 is subdued compared to SEDEX AI.

10. Halo model for the HYC deposit

A primary geochemical and mineralogical halo model has been developed for HYC (Fig. 14) based on the element dispersions and mineral chemistry data presented above for the three drill holes (Te 115, Barney 3 and BMR 2), combined with the previous studies of a further six drill holes by Lambert and Scott (1973). The major features of the halo model are as follows.

(1) An extensive Zn–Pb–Tl halo surrounds the deposit extending 250 m into the immediate hangingwall, but less than 50 m into the footwall. The halo extends along the favourable pyritic black shale facies at the base of the HYC Pyritic Shale for at least 15 km west to beyond DDH Barney 3. Sulphur in the form of pyrite is also enriched throughout most of the halo. The halo is characterised by values of Zn > 1000 ppm, Pb > 100 ppm and Tl > 4 ppm. The Tl halo may extend beyond the Zn–Pb halo into the hangingwall and footwall sediments but more data are required to test the full extent along strike.

(2) A ferroan dolomite/ankerite halo roughly coincides with the Zn–Pb–Tl halo but extends further into the footwall through the W-Fold Shale and into
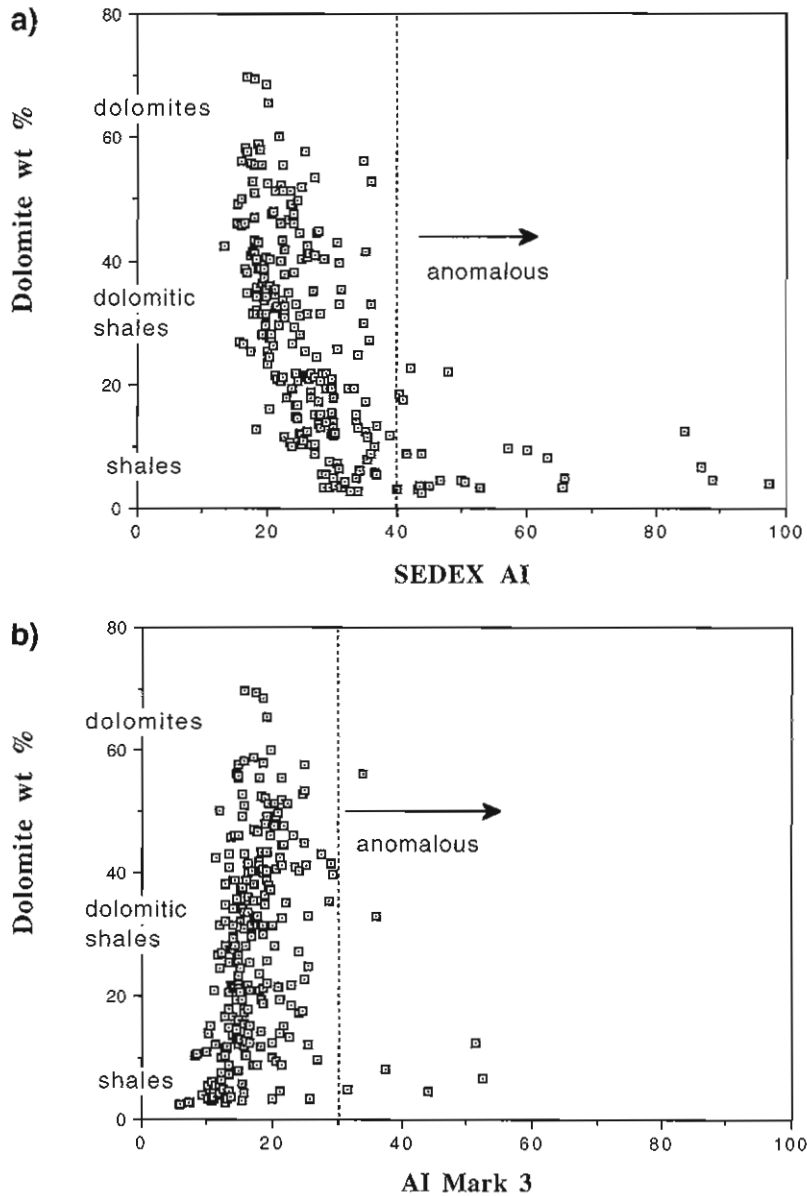
Fig. 12. (a, b) Variation of alteration index with dolomite content for a set of non-mineralised sediments from the McArthur Group. The samples plotted are a subset of sediments from the AGSO Rockchem database (Plumb et al., 1992). Note the trend of increasing SEDEX AI with decreasing dolomite content, termed the shale factor (a). This trend is reversed by using AI Mark 3 (b).

the Coxco Dolomite in the vicinity of the deposit. The most Fe-rich dolomites occur in the ore zone and along the base of the HYC Pyritic Shale.

(3) A Mn-carbonate halo (Mn–Fe dolomite and Mn-ankerite) tightly surrounds the deposit and extends along the W-Fold Shale Member for at least 23

km from HYC. Mn-carbonate is the most extensive halo expression of HYC extending well beyond the ankerite halo and the Zn–Pb–Tl halo. The calculated MnO content of dolomite within the halo (MnO_d) increases systematically toward the deposit along the W-Fold Shale from mean values of 0.75 wt% at 23
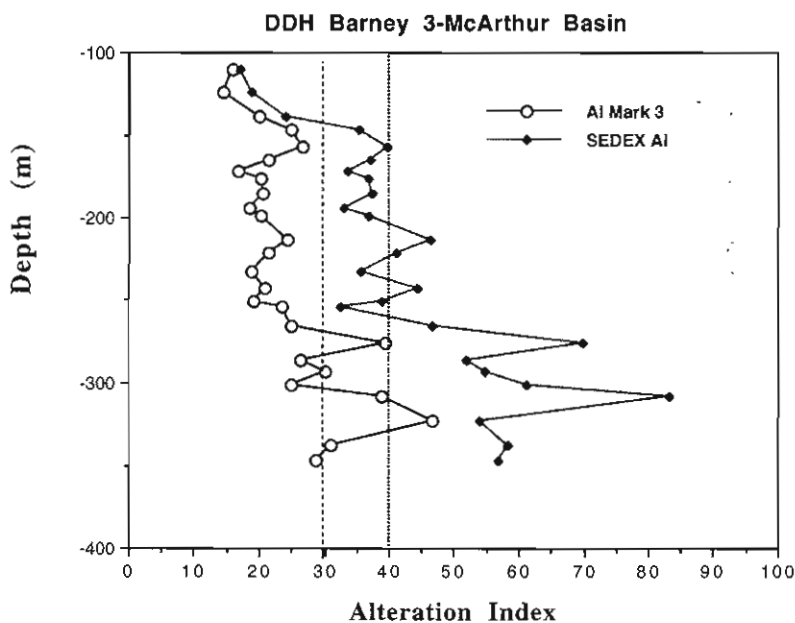
DDH Barney 3-McArthur Basin

Fig. 13. Comparison between SEDEX AI and AI Mark 3 in DDH Barney 3. The shale factor (see text) is removed by using AI Mark 3.

km distant, 1.5 wt% at 15 km distant to 8 wt% at the deposit. MnO_d also increases across strike to accurately define the footwall contact of the favourable unit.

(4) The alteration index adapted for Lady Loretta (SEDEX AI) and modified for the McArthur Basin (AI Mark 3) exhibits elevated values throughout the ferroan carbonate and manganiferous carbonate halos. Values of SEDEX AI > 60 and AI Mark 3 > 30 characterise these halos and mark the favourable unit.

10.1. Comparison of HYC and Lady Loretta halos

HYC and Lady Loretta are both Proterozoic stratiform Pb–Zn–Ag deposits within dolomite-bearing siltstone–shale sequences. Although they are vastly different in size (237 million tonnes compared with 8 million tonnes), they have very similar geochemical and mineralogical halos. Both deposits are surrounded by zones of Fe–Mn carbonate which roughly coincide with anomalous Zn, Pb and Tl. Manganese and Tl are the most laterally extensive along the favourable unit and the Mn content of sedimentary dolomite shows a systematic increase across strata towards the ore lenses in both cases. The major
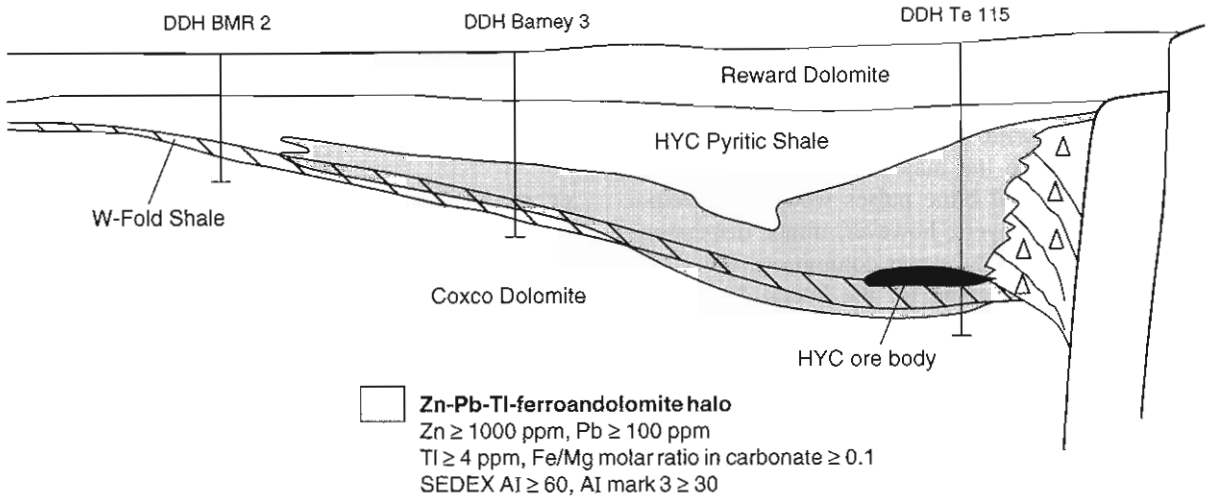
differences are that the HYC halo is much bigger than the Lady Loretta halo (15 km minimum lateral extent at HYC compared to ~2 km at Lady Loretta), and that siderite, which forms the inner halo carbonate at Lady Loretta, is lacking from the halo at HYC. At Lady Loretta the carbonate zonation away from the orebody is: ore → siderite → ankerite → ferroan dolomite → dolomite; whereas at HYC the zonation is: ore → ankerite → ferroan dolomite → dolomite.

10.2. Genetic considerations of halo formation

The extensive Mn-carbonate halo within the W-Fold Shale immediately below the HYC ore and correlative rocks is considered to be related to the release of cool Mn-bearing brines into the McArthur Basin during deepening of the basin (Large et al., 1998).

The W-Fold Shale represents a transitional facies between the shallow water Coxco Dolomite below, and the deeper water HYC Pyritic Shale above (Bull, 1998; Large et al., 1998). Manganese was deposited as Mn-carbonate within this transitional facies, where shallow oxidized basin fluids mixed with deeper reduced fluids in the depositional setting of the W-Fold Shale Member. The lack of Mn

a) Ferroan dolomite halo

Zn-Pb-Tl-ferroandolomite halo
Zn ≥ 1000 ppm, Pb ≥ 100 ppm
Tl ≥ 4 ppm, Fe/Mg molar ratio in carbonate ≥ 0.1
SEDEX AI ≥ 60, AI mark 3 ≥ 30

b) Manganese carbonate halo
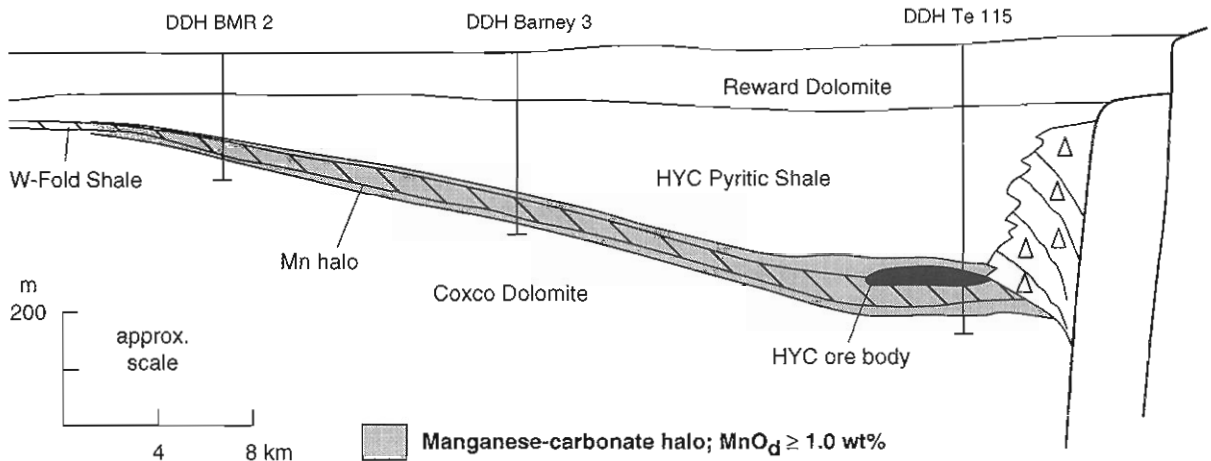

Manganese-carbonate halo; MnO$_d$ ≥ 1.0 wt%

Fig. 14. (a, b) Schematic cross-section showing interpreted lithogeochemical halos for the HYC deposit. Drill hole data used to compile this halo model are from Lambert and Scott (1973) and this study. The following holes are included: DDH Te 115, Ie 115, Ue 133, O 123, Barney 2, Barney 3, Wickens Hill, Myrtle 1 and BMR 2.

in the ore zone and upper HYC Pyritic Shale sequence suggests that the deep basin waters remained reduced throughout the period of ore formation and later shale sedimentation, thus allowing no opportunity for Mn deposition. Force and Maynard (1991) describe a similar environment for Mn-carbonate concentration along the margins of intra-continental basins such as the Black Sea.

The close spatial relationship between the Mn halo and the HYC deposit indicates that the release of Mn-brines into the basin, accompanying tectonic activity and basin deepening, signalled the start of the HYC hydrothermal event.

Previous studies by Williams (1978) and Hinman (1996) suggested that the HYC ore fluids were sourced from the north–south Emu and Western Faults and the related E–W faults to the north of the deposit. Large et al. (1998) suggest that the

ore fluids released from the faults were high-density concentrated brines that acted as bottom hugging currents moving downslope from the fault scarps to accumulate as a brine pool in the HYC sub-basin depocentre and precipitate successive layers of Zn–Pb accompanying pyritic black shale sedimentation.

In this scenario the majority of the Pb and Zn in the hydrothermal brine pulses would be precipitated in the ore layers; however, minor dispersion of base metals into the water column overlying the brine pool could account for the lateral dispersion of Zn, Pb and Tl in the coeval sediments at the base of the HYC Pyritic Shale regionally. In the Red Sea, Holmes and Tooms (1973) record widespread dispersion of Zn, Cu, Mn and Fe as both dissolved species and particulate matter in the normal seawater surrounding the Atlantas II Deep brine pool and associated metalliferous sediment deposit. This metal dispersion in the seawater has resulted in a geochemical halo of Mn, Zn and Cu developed in the sediments for up to 10 km from the brine pool and associated mineral deposit (Holmes and Tooms, 1973; Bignell et al., 1976) in an analogous manner to that recorded for HYC.

Following the main mineralising period at HYC, pyritic black shales continued to accumulate in the reduced deep water environment. The hangingwall halo of minor Zn–Pb throughout this sequence suggests that weaker brine exhalations continued from the Emu Fault system, but were probably cooler and relatively dilute compared to the main mineralising brines. The presence of the extensive pyrite and ferroan dolomite/ankerite halo surrounding HYC could be explained if these dilute exhalations were Fe-rich but base-metal-poor, the Fe being precipitated as diagenetic pyrite and ferroan dolomite/ankerite within organic-rich muds on and immediately below the basin floor.

In summary, the regional extent, geochemistry and mineralogy of the HYC halo is probably controlled by a number of factors.

(1) The water depth, sedimentary facies and redox basin floor conditions which control the precipitation and diagenetic growth of Mn-carbonate at the redox interface and pyrite and ankerite in the deeper water reduced black shale environment.

(2) The composition and temperature of the brine exhalations which controlled their density, brine pool development, and the concentration of dissolved Fe, Mn and base metals.

(3) Basin floor structure and architecture which controlled sub-basin development and the dispersion or confinement of exhaled brines.

11. Conclusions and significance for exploration

This study has shown that the halo model and exploration vectors developed for the Lady Loretta deposit have application, with minor modification, to the HYC deposit and McArthur Basin exploration. As might be expected for a giant deposit like HYC, the halo is very extensive, being traceable for 15 to 23 km west of the deposit.

Mn-carbonate forms the most extensive halo, and is best developed in the footwall sedimentary package immediately below the ore position. The calculated MnO content of sedimentary dolomite (MnO_d) has proved to be a very reliable vector to ore, increasing both stratigraphically and laterally in the proximity to mineralisation. Although an inner zone of siderite is not present at HYC, there is an extensive halo of ankerite/ferroan dolomite which is centred on the orebody and extends into the hangingwall pyritic shales and along strike from the ore deposit.

The SEDEX alteration index developed for Lady Loretta is also a useful vector for defining the favourable stratigraphic unit in the McArthur Basin. A modified index (AI Mark 3) is proposed which eliminates the effect of the shale/dolomite ratio on the index, and reduces the occurrence of false anomalies caused by 'barren shale' horizons.

11.1. Identification of favourable sedimentary units

The group of indices recommended for the identification of potential ore-bearing host units in the McArthur Basin, at a distance of about 10 to 20 km from ore, are outlined in Fig. 15 and listed below.

(1) MnO content of dolomite; $MnO_d > 1.0$ wt%. MnO_d increases stratigraphically from a background of about 0.3 wt% to a peak of 1.5 to 2.5 wt% over a distance of 20 to 50 m approaching the basal contact of the potential ore-bearing unit.

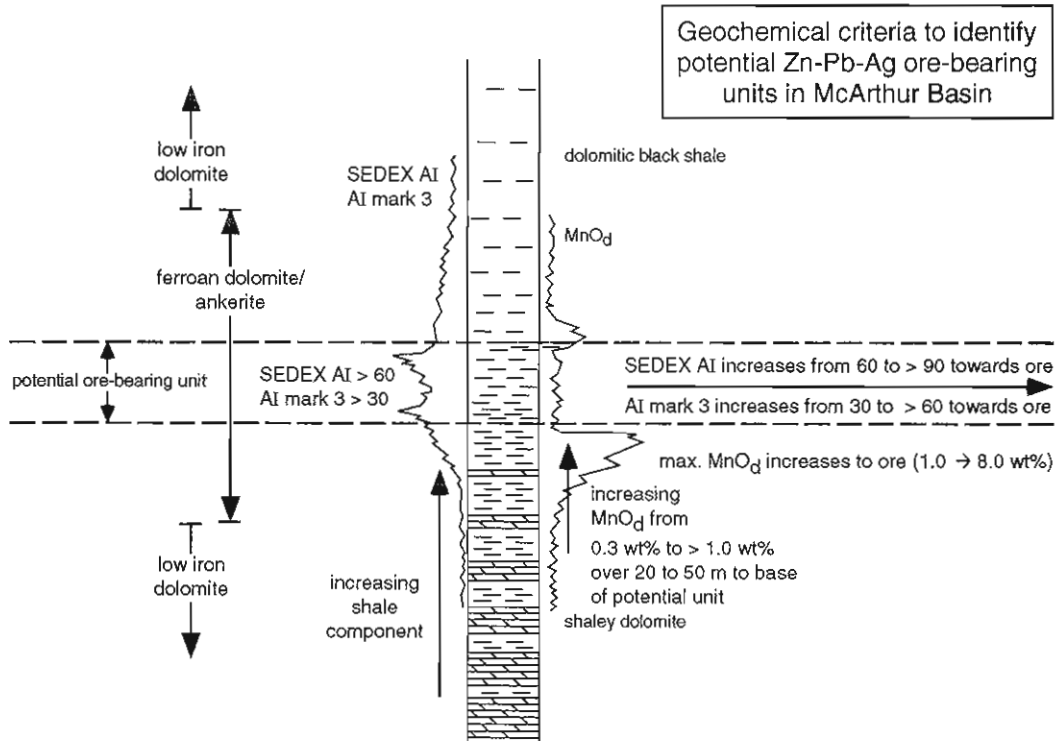(2) SEDEX AI > 60 and AI Mark 3 > 30 marks the favourable unit.

Fig. 15. Diagrammatic summary of geochemical criteria useful in the identification of potential ore-bearing units in the McArthur Basin. This diagram is not to scale as the potential unit may vary from 5 m to >100 m in thickness depending on proximity to the deposit.

(3) Tl > 4 ppm, Pb > 100 ppm, Zn > 1000 ppm.

(4) Metal index $Zn + 100 Pb + 100 Tl > 10^4$.

(5) Calculated carbonate molar ratio $Fe/Mg > 0.10$.

These indices are considered to have application in exploration for SEDEX Pb–Zn deposits in carbonate-bearing sedimentary basins.

References

Bignell, R.O., Cronan, D.S., Tooms, J.S., 1976. Metal dispersion in the Red Sea as an aid to marine geochemical exploration. Trans. Inst. Min. Metall. 85, B274–B278.

Brown, M.C., Claxton, C.W., Plumb, K.A., 1978. The Proterozoic Barney Creek Formation and some associated units of the McArthur Group, Northern Territory, Australia. Bureau of Mineral Resources, Canberra, Record, 1969/145, 59 pp.

Bull, S.W., 1998. Sedimentology of the Palaeoproterozoic Barney Creek formation in DDH BMR McArthur 2, Southern McArthur Basin, Northern Territory, Australia. Aust. J. Earth Sci. 45, 21–32.

Carr, G.R., 1984. Primary geochemical and mineralogical dispersion in the vicinity of the Lady Loretta Zn–Pb–Ag deposit, Northern Queensland. J. Geochem. Explor. 22, 217–238.

Corbett, J.A., Lambert, I.B., Scott, K.M., 1975. Results of anal-

yses of rocks from McArthur Area, Northern Territory, Australia. CSIRO Tech. Comm. 57, Minerals Research Laboratories, August, 35 pp.

Croxford, N.J.W., Jephcott, S., 1972. The McArthur lead–zinc–silver deposit, Northern Territory, Australia. Proc. Australas. Inst. Min. Metall. 243, 1–26.

Cruikshank, B.I., Pyke, J.G., 1993. Analytical methods used in Minerals and Land use Program's geochemical laboratory. Australian Geological Survey Organisation, Canberra, Rec. 1993/26, 22 pp.

Davidson, G.J., 1998. Alkali alteration styles and mechanisms, and their implications for a 'brine factory' source of base metals in the rift-related McArthur Group, Australia. Aust. J. Earth Sci. 45, 33–50.

Eldridge, C.S., Williams, N., Walshe, J.L., 1993. Sulfur isotope variability in sediment-hosted massive sulfide deposits as determined using the ion microprobe SHRIMP II: a study of the HYC Deposit at McArthur River, Northern Territory, Australia. Econ. Geol. 88, 1–26.

Force, E.R., Maynard, J.B., 1991. Manganese syngenetic deposits on the margins of anoxic basins. Rev. Econ. Geol. 5, 147–158.

Gustafson, L.B., Williams, N., 1981. Sediment-hosted stratiform deposits of copper, lead and zinc. Econ. Geol. 75, 139–178.

Hinman, M.C., 1995. Base metal mineralisation at McArthur River: structure and kinematics of the HYC-Cooley zone at McArthur River. Australian Geological Survey Organisation, Canberra, Rec. 1995/5, 29 pp.

Hinman, M., 1996. Constraints, timing and processes of stratiform base-metal mineralisation at the HYC Ag–Pb–Zn deposit, McArthur River (abstr.) — M.I.C. '96, New Developments in Metallogenic Research: The McArthur, Mt Isa, Cloncurry Minerals Province. Extended Abstr., EGRU Contrib. 56, Townsville, pp. 56–59.

Holmes, R., Tooms, J.S., 1973. Dispersion from a submarine exhalative body. In: Jones, M.J. (Ed.), Geochemical Exploration 1972. Institute of Mining and Metallurgy, London, pp. 193–202.

Lambert, I.B., 1976. The McArthur lead–zinc–silver deposit: features in metagenesis and comparisons with some other stratiform ores. In: Wolfe, K.H. (Ed.), Handbook of Stratabound and Stratiform Ore Deposits, 6. Elsevier, Amsterdam, pp. 535–585.

Lambert, I.B., Scott, K.M., 1973. Implications of geochemical investigations of sedimentary rocks within and around the zinc–lead–silver deposit, Northern Territory, Australia. J. Geochem. Explor. 2, 307–330.

Large, R.R., McGoldrick, P.J., 1998. Lithogeochemical halos and geochemical vectors to stratiform sediment hosted Zn–Pb–Ag deposits, Part 1. Lady Loretta deposit, Queensland. J. Geochem. Explor. 63, 37–56.

Large, R.R., Bull, S.W., Cooke, D.R., McGoldrick, P.J., 1998. A genetic model for the HYC deposit, Australia: based on regional sedimentology, geochemistry and sulfide–sediment relationships. Econ. Geol. 93, 1345–1368.

Logan, R.G., 1979. The Geology and Mineralogical Zoning of the HYC Ag–Pb–Zn Deposit, McArthur River, Northern Territory, Australia. Unpubl. MSc Thesis, Australian National University, Research School of Earth Sciences, Canberra, 187 pp.

Plumb, K.A., Wyborn, L.A.I., Ryburn, R.J., 1992. McArthur Basin and Murphy Inlier Rockchem dataset documentation. Bureau of Mineral Resources, Canberra, Record 1992/37, 34 pp.

Smith, R.N., 1973. Trace Element Distributions within some Major Stratiform Orebodies. Unpubl. BSc (Hons) Thesis, University of Melbourne.

Walker, R.N., Logan, R.G., Binnekamp, J.G., 1977. Recent geological advances concerning the HYC and associated deposits, McArthur River, Northern Territory, Australia. J. Geol. Soc. Aust. 24, 365–380.

Williams, N., 1978. Studies of the base-metal sulfide deposits at McArthur River, Northern Territory, Australia, I. The Cooley and Ridge deposits. Econ. Geol. 73, 1005–1035.